nors, although it was reported that some lepromatous leprosy patients have a mutation in the intracellular domain of TLR2 (2, 11). Furthermore, DC pulsed with recombinant MMP-II successfully stimulated T cells from lepromatous leprosy patients to produce IFN-γ to the same level as that produced by healthy donors. Therefore, BCG-SM may be useful for stimulating T cells in lepromatous leprosy patients and for controlling bacterial spread (19). The combination of priming with a more immunostimulatory BCG strain, such as a recombinant BCG strain secreting an immunodominant protein (for example, BCG-SM), and boosting with a recombinant protein, such as MMP-II, may provide more powerful immunostimulatory measures against *M. leprae* infection. Further study should be pursued to evaluate the protective activity of BCG-SM against leprosy.

ACKNOWLEDGMENTS

We acknowledge the contribution of N. Makino in the preparation of the manuscript. We also thank Y. Harada for her technical support and the Japanese Red Cross Society for kindly providing PBMC from healthy donors.

This work was supported in part by a grant-in-aid for Research on Emerging and Re-Emerging Infectious Diseases and by a grant-in-aid for Research on HIV/AIDS from the Ministry of Health, Labor, and Welfare of Japan.

REFERENCES

1. **Blander, S. J., L. Szeto, H. A. Shuman, and M. A. Horwitz.** 1990. An immunoprotective molecule, the major secretory protein of Legionella pneumophila, is not a virulence factor in a guinea pig model of Legionnaires' disease. J. Clin. Investig. **86**:817–824.
2. **Bochud, P. Y., T. R. Hawn, and A. Aderem.** 2003. Cutting edge: a Toll-like receptor 2 polymorphism that is associated with lepromatous leprosy is unable to mediate mycobacterial signaling. J. Immunol. **170**:3451–3454.
3. **Grange, J. M.** 1998. Complications of bacille Calmette-Guerin (BCG) vaccination and immunotherapy and their management. Commun. Dis. Public Health **1**:84–88.
4. **Grode, L., P. Seiler, S. Baumann, J. Hess, V. Brinkmann, A. N. Eddine, P. Mann, C. Goosmann, S. Bandermann, D. Smith, G. J. Bancroft, J.-M. Reyrat, D. van Soolingen, B. Raupach, and S. H. E. Kaufmann.** 2005. Increased vaccine efficacy against tuberculosis of recombinant *Mycobacterium bovis* bacille Calmette-Guerin mutants that secrete listeriolysin. J. Clin. Investig. **115**:2472–2479.
5. **Hagge, D. A., N. A. Ray, J. L. Krahenbuhl, and L. B. Adams.** 2004. An in vitro model for the lepromatous leprosy granuloma: fate of *Mycobacterium leprae* from target macrophages after interaction with normal and activated effector macrophages. J. Immunol. **172**:7771–7779.
6. **Harth, G., B. Y. Lee, and M. A. Horwitz.** 1997. High-level heterologous expression and secretion in rapidly growing nonpathogenic mycobacteria of four major *Mycobacterium tuberculosis* extracellular proteins considered to be leading vaccine candidates and drug targets. Infect. Immun. **65**:2321–2328.
7. **Hashimoto, K., Y. Maeda, H. Kimura, K. Suzuki, A. Masuda, M. Matsuoka, and M. Makino.** 2002. *Mycobacterium leprae* infection in monocyte-derived dendritic cells and its influence on antigen-presenting function. Infect. Immun. **70**:5167–5176.
8. **Horwitz, M. A., G. Harth, B. J. Dillon, and S. Maslesa-Galic.** 2000. Recombinant bacillus Calmette-Guerin (BCG) vaccines expressing the *Mycobacterium tuberculosis* 30-kDa major secretory protein induce greater protective immunity against tuberculosis than conventional BCG vaccines in a highly susceptible animal model. Proc. Natl. Acad. Sci. USA **97**:13853–13858.
9. **Horwitz, M. A., B. W. Lee, B. J. Dillon, and G. Harth.** 1995. Protective immunity against tuberculosis induced by vaccination with major extracellular proteins of *Mycobacterium tuberculosis*. Proc. Natl. Acad. Sci. USA **92**:1530–1534.
10. **Jiao, X., R. Lo-Man, P. Guermonprez, L. Fiette, E. Deriaud, S. Burgaud, B. Gicquel, N. Winter, and C. Leclerc.** 2002. Dendritic cells are host cells for mycobacteria in vivo that trigger innate and acquired immunity. J. Immunol. **168**:1294–1301.
11. **Kang, T. J., and G. T. Chae.** 2001. Detection of Toll-like receptor 2 (TLR2) mutation in the lepromatous leprosy patients. FEMS Immunol. Med. Microbiol. **31**:53–58.
12. **Kaufmann, S. H. E., and A. J. McMichael.** 2005. Annulling a dangerous liaison: vaccination strategies against AIDS and tuberculosis. Nat. Med. **11**:S33–S44.
13. **Krutzik, S. R., B. Tan, H. Li, M. T. Ochoa, P. T. Liu, S. E. Sharfstein, T. G. Graeber, P. A. Sieling, Y.-J. Liu, T. H. Rea, B. R. Bloom, and R. L. Modlin.** 2005. TLR activation triggers the rapid differentiation of monocytes into macrophages and dendritic cells. Nat. Med. **11**:653–660.
14. **Liu, Y. J.** 2001. Dendritic cell subsets and lineages, and their functions in innate and adaptive immunity. Cell **106**:259–262.
15. **Lombardi, C., E. S. Pedrazzani, J. C. Pedrazzani, P. F. Filho, and F. Zicker.** 1996. Protective efficacy of BCG against leprosy in San Paulo. Bull. Pan Am. Health Organ. **30**:24–30.
16. **Maeda, S., M. Matsuoka, N. Nakata, M. Kai, Y. Maeda, K. Hashimoto, H. Kimura, K. Kobayashi, and Y. Kashiwabara.** 2001. Multidrug resistant *Mycobacterium leprae* from patients with leprosy. Antimicrob. Agents Chemother. **45**:3635–3639.
17. **Maeda, Y., T. Mukai, J. Spencer, and M. Makino.** 2005. Identification of immunomodulating agent from *Mycobacterium leprae*. Infect. Immun. **73**:2744–2750.
18. **Makino, M., and M. Baba.** 1997. A cryopreservation method of human peripheral blood mononuclear cells for efficient production of dendritic cells. Scand. J. Immunol. **45**:618–622.
19. **Makino, M., Y. Maeda, and N. Ishii.** 2005. Immunostimulatory activity of major membrane protein-II from *Mycobacterium leprae*. Cell. Immunol. **233**:53–60.
20. **Makino, M., S. Shimokubo, S. Wakamatsu, S. Izumo, and M. Baba.** 1999. The role of human T-lymphotropic virus type 1 (HTLV-1)-infected dendritic cells in the development of HTLV-1-associated myelopathy/tropical spastic paraparesis. J. Virol. **73**:4575–4581.
21. **Pessolani, M. C., E. R. Smith, B. Rivoire, J. McCormick, S. A. Hefta, S. T. Cole, and P. J. Brennan.** 1994. Purification, characterization, gene sequence, and significance of a bacterioferritin from *Mycobacterium leprae*. J. Exp. Med. **180**:319–327.
22. **Ponnighaus, J. M., P. E. Fine, J. A. Sterne, R. J. Wilson, E. Msosa, P. J. Gruer, P. A. Jenkins, S. B. Lucas, N. G. Liomba, and L. Bliss.** 1992. Efficacy of BCG vaccine against leprosy and tuberculosis in northern Malawi. Lancet **14**:636–639.
23. **Ridley, D. S., and W. H. Jopling.** 1966. Classification of leprosy according to immunity. A five-group system. Int. J. Lepr. Other Mycobact. Dis. **34**:255–273.
24. **Sambrook, J., and D. W. Russell.** 2001. Molecular cloning: a laboratory manual, 3rd ed. Cold Spring Harbor Laboratory Press, Cold Spring Harbor, N.Y.
25. **Sharma, P., R. Mukherjee, G. P. Talwar, K. G. Sarathchandra, R. Walia, S. K. Parida, R. M. Pandey, R. Rani, H. Kar, A. Mukherjee, K. Katoch, S. K. Benara, T. Si, and P. Singh.** 2005. Immunoprophylactic effects of the anti-leprosy *Mw* vaccine in household contacts of leprosy patients: clinical field trials with a follow up of 8–10 years. Lepr. Rev. **76**:127–143.
26. **Sieling, P. A., D. Jullien, M. Dahlem, T. F. Tedder, T. H. Rea, R. L. Modlin, and S. A. Porcelli.** 1999. CD1 expression by dendritic cells in human leprosy lesions: correlation with effective host immunity. J. Immunol. **162**:1851–1858.
27. **Snapper, S. B., L. Lugosi, A. Jekkel, R. E. Melton, T. Kieser, B. R. Bloom, and W. R. Jacobs, Jr.** 1988. Lysogeny and transformation in mycobacteria: stable expression of foreign genes. Proc. Natl. Acad. Sci. USA **85**:6987–6991.
28. **Wakamatsu, S., M. Makino, C. Tei, and M. Baba.** 1999. Monocyte-driven activation-induced apoptotic cell death of human T-lymphotropic virus type I-infected T cells. J. Immunol. **163**:3914–3919.
29. **Winau, F., S. Weber, S. Sad, J. de Diego, S. L. Hoops, B. Breiden, K. Sandhoff, V. Brinkmann, S. H. E. Kaufmann, and U. E. Schaible.** 2006. Apoptotic vesicles crossprime CD8 T cells and protect against tuberculosis. Immunity **24**:105–117.
30. **World Health Organization.** 2003. Leprosy elimination campaigns: impact on case detection. Wkly. Epidemiol. Rec. **78**:9–16.

Editor: W. A. Petri, Jr.

JSHC
Japan Society of Histochemistry and Cytochemistry
Established 1953

Acta Histochem. Cytochem. 39 (4): 107–112, 2006
doi:10.1267/ahc.06010

Localization of CORO1A in the Macrophages Containing *Mycobacterium leprae*

Koichi Suzuki[1,2], Fumihiko Takeshita[1,3], Noboru Nakata[1], Norihisa Ishii[2] and Masahiko Makino[1]

[1]Department of Microbiology and [2]Department of Bioregulation, Leprosy Research Center, National Institute of Infectious Diseases, 4–2–1 Aoba-cho, Higashimurayama, Tokyo 189–0002, Japan, and the [3]Department of Molecular Biodefense Research, Yokohama City University School of Medicine, 3–9 Fukuura, Kanazawa-ku, Yokohama 236–0004, Japan

Received April 19, 2006; accepted June 1, 2006; published online June 28, 2006

Mycobacteria have acquired an intracellular lifestyle within the macrophage, which is best exemplified by the enlarged infected histiocytes seen in lepromatous leprosy. To survive within the cell, mycobacteria must escape intracellular bactericidal mechanisms. In a study of *Mycobacterium bovis* Bacille Calmette-Guérin (*M. bovis* BCG) infection, it was shown that the host protein, CORO1A, also known as tryptophan aspartate-containing coat protein (TACO), accumulates on the phagosomal membrane, resulting in inhibition of phagosome-lysosome fusion, and thus augmenting intracellular survival. In this study, we show that CORO1A strongly localizes on the membrane of phagosomes that contain *Mycobacterium leprae* (*M. leprae*), where Toll-like receptor 2 was also visualized by immunostaining. When cultured macrophages were infected with *M. leprae*, CORO1A recruitment from the plasma membrane to the phagosomal membrane was observed. Moderate to strong CORO1A retention was observed in late lesions that contained foamy histiocytes, in which *M. leprae* were difficult to detect by acid-fast staining. These results suggest that components accumulating within the phagosome rather than viable bacilli are responsible for the retention of CORO1A, and that there is also a bactericidal mechanism in the macrophage that might counter the effects of CORO1A.

Key words: *Mycobacterium leprae*, macrophage, phagosome, CORO1A, Toll-like receptor

I. Introduction

The adoption of an intracellular lifestyle confers several advantages on microbial pathogens: they are inaccessible to humoral and complement-mediated immune attack; they no longer require a specific adherence mechanism to maintain their site of infection; and they have accessibility to a range of nutrients. However, in order for mycobacteria to survive intracellularly, they also need to escape from intracellular bactericidal mechanisms.

Mycobacterium leprae (*M. leprae*) is one of the most successful intracellular pathogens, surviving within the phagosome of host macrophages. Such intracellular parasitization is most readily seen in the histiocytic lesions of lepromatous leprosy, which are characterized by an accumulation of histiocytes (termed leproma cells). They have enlarged phagosomes in which *M. leprae* lives and replicates. Because these phagosomes remain unfused with lysosomes, degradation of bacilli by bactericidal enzymes is prevented, resulting in their survival [8].

An *in vitro* study using *Mycobacterium bovis* Bacille Calmette-Guérin (*M. bovis* BCG) demonstrated that an important host protein, termed tryptophan aspartate-containing coat protein (TACO), plays an essential role in the inhibition of phagosome-lysosome fusion, as well as in the survival of bacilli within macrophages [7]. In the mouse macrophage cell line, J774.1, it was shown that TACO, which initially was found on the plasma membrane in association with tubulin, was recruited to the phagosomal membrane following infection by *M. bovis* BCG [7]. TACO represents a component of the phagosome coat, and retention of TACO prevents phagosomes from fusing with lysosomes, thereby contributing to the long-term survival of bacilli

Correspondence to: Koichi Suzuki, Department of Bioregulation, Leprosy Research Center, National Institute of Infectious Diseases, 4–2–1 Aoba-cho, Higashimurayama, Tokyo 189–0002, Japan.
E-mail: koichis@nih.go.jp.

within the phagosome. The phagosomal localization of TACO was only transient in macrophages engulfing dead mycobacteria, whereas localization was quite stable when live bacilli were used. In addition, *M. bovis* BCG was completely digested in liver Kupffer cells, which lack TACO expression [7]. Mouse TACO is an ortholog of human CORO1A, also known as p57 [13], which encodes a 461-amino acid protein, that shares 40% amino acid identity with coronin, an actin-binding protein of the cellular slime mold *Dictyostelium discoideum* [6]. CORO1A actually binds to actin [13], and is thought to be important for cell mobility and endocytic activity, since it accumulates in cortical sites of moving cells and contributes to the dynamics of the intracellular actin system [6].

Macrophages and other immune cells have evolved several mechanisms to detect and combat pathogens. Among these mechanisms, toll like receptors (TLRs) are the pattern recognition receptors (PRRs) that sense and distinguish various components derived from pathogens, *i.e.* pathogen-associated molecular patterns (PAMPs) [1, 4]. TLR2 in combination with TLR1 or TLR6 are the most important for recognition of mycobacteria [10, 18], and bacterial lipopeptides, such as lipoarabinomannan (LAM), are well-known ligands for TLR2. Notably, several studies have demonstrated that TLR2 is recruited and localized on the phagosome membrane following exposure to its ligands, such as zymosan [17].

It is not known whether the observations regarding TACO activity that enhanced the survival of *M. bovis* BCG are universal for other mycobacteria, especially *in vivo*. In this study we investigate the expression and localization of CORO1A in macrophages infected with *M. leprae* both *in vivo* and *in vitro*.

II. Materials and Methods

Tissue samples and staining

Archived formalin-fixed, paraffin-embedded tissue sections from 42 cases of leprosy patients were subjected to immunohistochemical staining as described [12, 15]. Briefly, deparaffinized sections were incubated with rabbit anti-TACO antibody [7], which is specific for both mice and human CORO1A, was kindly provided by Dr. J. Pieters (Basel Institute for Immunology, Basel, Switzerland), rabbit anti-human Toll-like receptor 2 (TLR2) antibody (Santa Cruz Biotechnology, Santa Cruz, CA) or with anti-lipoarabinomannan (LAM) antibody (LRC, National Institute of Infectious Diseases, Japan), for 1 hr at room temperature. Slides were washed with Dulbecco's phosphate buffered saline (DPBS) containing 0.01% Triton X-100. The peroxidase- or alkaline phosphatase-labeled streptavidin-biotin method using the LSAB2 kit (DAKO, Carpinteria, CA) and DAB (3,3-diaminobenzidine tetrahydrochloride) or BCIP/NBT (5'-bromo-4-chloro-3-indoxyl phosphate/nitro blue tetrazolium chloride) was employed according to the manufacturer's protocol. Sections were then stained using carbol fuchsin to visualize acid-fast mycobacteria and counter-stained with hematoxylin. For the Fite method of Ziehl-Neelsen staining, olive oil/xylene (1:2 ratio) was used to deparaffinize sections. Archived formalin-fixed, paraffin-embedded tissues were used according to the guidelines approved by the National Institute of Infectious Diseases (Tokyo, Japan).

Macrophage cell culture and M. leprae infection

Murine macrophage cell lines, RAW264.7, P388D1, and J774.1, were obtained from the American Type Culture Collection (ATCC; Manassas, VA). They were maintained in Dulbecco's Modified Eagle Medium (DMEM) supplemented with 10% fetal calf serum (FCS) and 50 mg/ml penicillin/streptomycin at 37°C in 5% CO_2. Peritoneal resident macrophages were harvested from Balb/c mice as previously described [9]. Briefly, peritoneal cells were recovered in Hanks' balanced salt solution (HBSS), washed, suspended in DMEM supplemented with 15% FBS, and plated on glass coverslips in 24 well tissue culture plates. After 4 hr incubation, unadhered cells were removed by gentle rinsing with HBSS. *M. leprae* was prepared from footpads of nude mice as described [9] and added to the culture at a multiplicity of infection (MOI) of 20:1.

RNA preparation and Northern blot analysis

RNA from cultured macrophages was prepared using RNeasy Mini Kits (QIAGEN Inc., Valencia, CA) and minor modifications of the manufacturer's protocol as described [14, 16]. Briefly, cells were washed with DPBS, resuspended in 600 μl of Lysis solution, and passed through a QIAshredder (QIAGEN). After 600 μl of 70% ethanol was added, the mixture was purified through a spin column, washed with 600 μl of RW1 wash solution, and washed twice with 500 μl of RPE wash solution. RNA was eluted with 30 μl of RNase-free water. RNA samples were electrophoresed on denaturing agarose gels and capillary blotted on a nylon membrane using a Turboblotter (Schleicher & Schuell, Keene, NH). After UV cross-linking, hybridization was performed as follows. cDNA probes were labeled with ^{33}P-dCTP using a *Bca*BEST Labeling Kit (Takara Bio, Otsu, Japan). After the Nytran membranes (Schleicher & Schuell) were prehybridized with 10 ml of QuickHyb Hybridization Solution (Stratagene) for 1 hr at 68°C, 1×10^7 cpm radiolabeled probe was added after it had been premixed with 100 μl sonicated salmon sperm DNA (Stratagene), heated at 94°C for 5 min, and then chilled on ice. After hybridization for 3 hr, membranes were washed and analyzed using a BAS1000 BioImaging analyzer (Fujifilm, Tokyo, Japan). Reprobing was performed after incubating membranes in 50% formamide, 50 mM Tris-Cl (pH 8.0), and 10% SDS for 1 to 2 hr at 65°C. Mouse CORO1A cDNA was obtained by RT-PCR using primers 5'-ACCTCCTGCCGTGACAAGCG-3' and 5'-TCCTGGAACAGGTCCGACTTTC-3'.

III. Results

Intracellular parasitization by mycobacteria is best

exemplified in lepromatous leprosy. The most characteristic feature of lepromatous leprosy is the dermal lesion, containing an accumulation of foamy histiocytes within enlarged phagosomes that contain acid-fast bacilli (*M. leprae*) (Fig. 1A and B). In order to study subcellular localization of CORO1A in such macrophages, skin biopsy specimens from patients with lepromatous leprosy were immunostained for CORO1A. As shown in Figure 1C and D, CORO1A localized to the phagocytic vacuoles containing *M. leprae*. Of note, there did not appear to be a direct association between bacilli and CORO1A, which were separated by lipids accumulated within the phagocytic vacuole (Fig. 1C and D). Phagosomal localization of CORO1A was confirmed by immunostaining serial sections of skin biopsy specimens for TLR2, which is known to localize on phagosomal membranes that contain mycobacteria, and which is responsible for initiation of innate immune responses [17, 18]. In the skin lesions of lepromatous leprosy, CORO1A localized to the same histiocytic lesion where TLR2 was also stained as shown in low magnification (Fig. 1E and F, respectively). In higher magnification, both were localized to the phagocytic vacuoles containing *M. leprae* (Fig. 1G and H).

Tuberculoid leprosy is characterized by strong cellular immune responses against *M. leprae*, accompanied by the appearance of epithelioid cells and giant cells (Fig. 1I). In biopsies of tuberculoid leprosy lesions, *M. leprae* was infrequently detected either by Fite staining or immunostaining of LAM, a component of the mycobacterial cell wall (negative staining shown in Fig. 1J and K, respectively). CORO1A expression in tissue macrophages was only weakly detected on the plasma membrane and cytoplasm in tuberculoid leprosy (Fig. 1L).

Foamy histiocytes in late lesions from lepromatous leprosy sometimes have a xanthomatous appearance, as demonstrated in Figure 2A, and acid-fast bacilli were not observed because of degenerative changes (Fig. 2C). However, CORO1A was rather strongly immunostained in such lesions (Fig. 2E). Positive immunostaining of LAM, which persists for a long period of time within infected macrophages, confirmed the preexistence of *M. leprae* in these foamy macrophages (Fig. 2G). In a different lesion within the same tissue section (Fig. 2B), both CORO1A staining and LAM staining were relatively weak (Fig. 2F and H, respectively), in spite of the existence of numerous acid-fast bacilli (Fig. 2D). These results, together with the observation that there was no direct association between bacilli

Fig. 1. Histopathological characterization of the skin lesions of leprosy. Hematoxylin and eosin staining of a tissue section from lepromatous leprosy shows accumulation of histiocytes in the dermis (**A**). Fite staining reveals numerous bacilli stained with pink coloration within the histiocytes (**B**). Immunostaining for CORO1A, shown as brown coloration, followed by acid-fast staining and hematoxylin counterstaining (**C** and **D**). Immunostaining for CORO1A (**E** and **G**), and for TLR2 (**F** and **H**), followed by acid-fast staining and hematoxylin counterstaining (both **E** and **F**, and **G** and **H**, are serial sections). Phagosomal membrane was visualized by light brown coloration in these figures and pink bacilli can be recognized in each phagocytic vacuole. Sections from a skin biopsy from tuberculoid leprosy were subjected to hematoxylin and eosin staining (**I**), Fite staining (**J**), LAM immunostaining (**K**) and CORO1A immunostaining (**L**). Both Fite and LAM staining were negative, and CORO1A staining was weakly visualized to the plasma membrane of histiocytes. Original magnification: ×100 (**A, B, E** and **F**; Bars=100 μm); ×200 (**G, H, I, J, K** and **L**; Bar=20 μm); ×400 (**C** and **D**; Bar=20 μm).

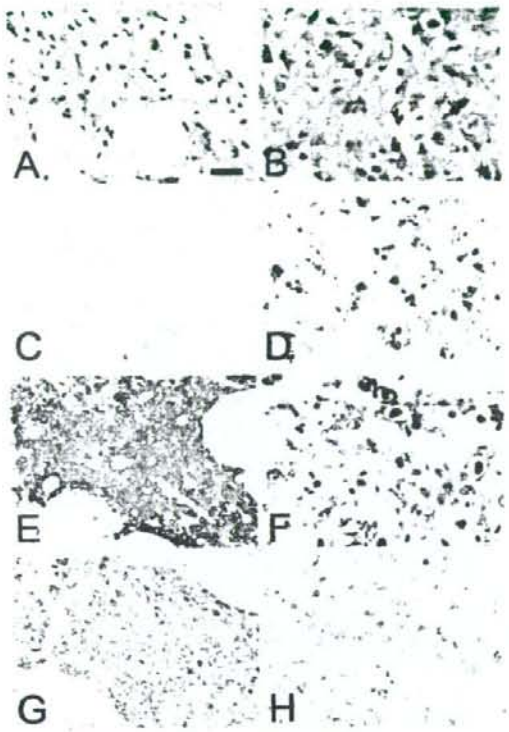

Fig. 2. Accumulation of CORO1A on phagosomal membranes is independent of the existence of live bacilli. Serial sections of a skin biopsy from lepromatous leprosy were subjected to hematoxylin and eosin staining (**A** and **B**), Fite staining (**C** and **D**), CORO1A immunostaining (**E** and **F**) and LAM immunostaining (**G** and **H**). Photomicrographs of **A, C, E** and **G** are taken from the same area, and **B, D, F** and **H** are from a different area within the same specimen. Original magnification: ×200. Bar=20 μm.

and CORO1A, as shown in Figure 1G and H, suggest that products from *M. leprae* accumulate within the phagosome, and that these components, and not necessarily the direct interaction of the phagosomal membrane with live bacilli, might be important for the retention of CORO1A on the phagosomal membrane.

To confirm the localization of CORO1A *in vitro*, murine peritoneal macrophages were infected with *M. leprae*, and the infected cells were fixed with formalin, immunostained for CORO1A, and then stained for acid-fast bacilli. CORO1A was initially distributed on the plasma membrane of the macrophage (Fig. 3A). However, 4 hr after infection it relocalized to phagosomal membranes containing *M. leprae* (Fig. 3B, C and D). Of note, some engulfed bacilli were observed in which there was no recruitment of CORO1A to the phagosomal membrane (Fig. 3C and D, arrows), which has been reported previously [11].

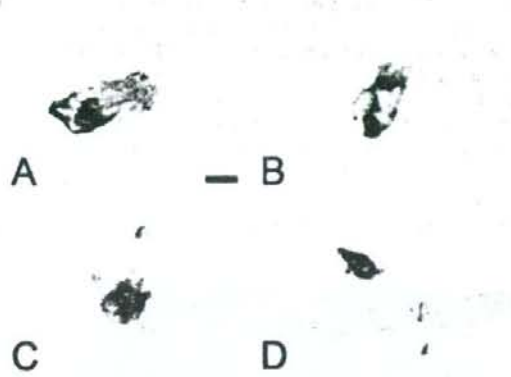

Fig. 3. CORO1A localization in the mouse peritoneal macrophage *in vitro*. Macrophages grown on cover slips were infected with *M. leprae* and subjected to CORO1A immunostaining, shown as dark coloration of BCIP/NBT, followed by acid-fast staining. Macrophages before infection of *M. leprae* (**A**) and those from 4 hr after infection (**B, C** and **D**). Arrows indicate *M. leprae* without a CORO1A coat around phagosomes. Original magnification: ×400. Bar=10 μm.

In addition to changes in subcellular localization, the pattern of CORO1A immunostaining suggested possible changes in its expression level following *M. leprae* infection. We therefore examined changes in CORO1A RNA levels following *M. leprae* infection, using three independent macrophage cell lines. Northern blot analysis revealed that mRNA levels were decreased 4 hr after *M. leprae* infection, and then gradually recovered by 48 hr to levels that were similar or slightly increased over the levels seen before infection (Fig. 4). Such a tendency was observed similarly in the three different macrophage cell lines tested.

IV. Discussion

Despite the fact that the macrophage is one of the most important immune cells protecting the body from infection, pathogenic mycobacteria such as *M. tuberculosis* and *M. leprae* parasitize the macrophage by evading its intracellular killing mechanisms. In this regard, the lepromatous leprosy lesion is the most classic example demonstrating intracellular parasitization of mycobacteria within the macrophage. It has been shown in the murine model of mycobacterial infection that TACO, the mouse CORO1A ortholog, accumulates in phagosomes containing mycobacteria and inhibits their fusion with lysosomes. Therefore, CORO1A has been considered as an essential host protein that permits the intracellular survival of mycobacteria [7], although the molecular mechanisms underlying such a function of CORO1A is still unknown.

In this study we demonstrated for the first time that CORO1A localizes on phagosomal membranes containing *M. leprae* in tissue specimens from lepromatous leprosy

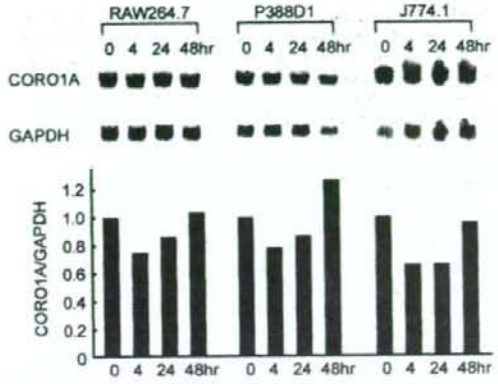

Fig. 4. Changes in CORO1A mRNA expression following *M. leprae* infection. Murine macrophage cell lines RAW264.7, P388D1, and J774.1 were utilized. Cells (5×10^5) were cultured in 10 cm dishes and infected with 5×10^6 organisms of *M. leprae*. After incubation for the indicated time, total RNA was obtained, and Northern blot analysis was performed as described in Materials and Methods. The density of each band was evaluated using Fuji Image Gauge software, and normalized to the mRNA levels of glyceraldehyde-3-phosphate dehydrogenase (GAPDH). Ratios relative to the original levels are shown in bar graphs below each Northern blot. CORO1A mRNA levels relative to GAPDH decreased in 4 hr following infection and recovered to the original levels in 48 hr. The same experiments were repeated three times using different batches of cells, and the typical results for each were presented.

patients. Because *M. leprae* cannot be cultivated *in vitro*, it is not possible to directly determine the contribution of CORO1A to *M. leprae* survival. In the study of *M. bovis* BCG infection, however, it was clearly shown that the existence of CORO1A enhances intracellular survival of bacilli [7]. Therefore, the observed accumulation of CORO1A around phagocytic vacuoles that contained *M. leprae* strongly indicates that CORO1A is a factor in the pathogenesis of leprosy. After translocation to the phagocytic vacuole, stable retention of CORO1A occurred only when viable, but not inactivated *M. bovis* BCG (killed by either heat or antibiotics) was engulfed [7]. It was shown that phagosomes containing bacterial clumps, rather than individual or low numbers of *M. bovis* BCG, are required for CORO1A retention [11]. *M. leprae* infection as shown in Figure 4 in this study supports that observation. Thus, it may be possible that individual isolated bacilli, are processed by a different phagocytic pathway. Another possibility for the lack of CORO1A accumulation on some phagosomes is the low viability of *M. leprae* prepared from nude mice, because CORO1A is not maintained on phagosomes that engulf dead bacilli [7]. Using the freeze-substitution method in electron microscopy, Amako *et al.* performed ultrastructural studies of *M. leprae* freshly prepared from nude mice footpads, and reported that most bacilli were degraded [2].

Although the mycobacterial factor that contributes to the anchoring of CORO1A has not yet been determined, it has been observed in *Helicobacter pylori* strains that the vacuolating cytotoxin, VacA, plays an important role in the retention of CORO1A, as well as in the interruption of lysosomal fusion [19]. In leproma cells, bacilli appeared to be floating in lipid-filled phagosomes, and therefore direct association between *M. leprae* and CORO1A was not evident. Moreover, CORO1A accumulation on phagosomal membranes seemed to be stronger in late lesions where viable bacilli were not present. These results suggest that, rather than the existence of live bacilli, some component accumulating in the phagosome contributes to the retention of CORO1A. It may also suggest that for these late lesions the bactericidal mechanism was effective despite the CORO1A coat on the phagosomal membrane.

An interesting observation is that both CORO1A and TLR2 localize on the phagosomal membrane containing *M. leprae*. TLR2 activates the innate immune response for protecting cells against pathogens [18], while CORO1A inhibits fusion of the lysosome to the phagosome, allowing mycobacterial parasitization [7]. The Arg677Trp polymorphism of TLR2, which is unable to initiate downstream signaling cascades, has been reported to be associated with lepromatous leprosy [5], as well as tuberculosis [3]. Within the infected macrophage both mycobacteria-killing and mycobacteria-tolerant mechanisms, mediated at least in part by TLR2 and CORO1A, respectively, may be activated. The balance between such competing mechanisms might be one factor in determining whether the pathogen is killed or instead parasitizes the host macrophage.

V. Acknowledgments

The authors thank Dr. J. Pieters (Basel Institute for Immunology, Basel, Switzerland), for the rabbit anti-TACO antibody. We also thank Dr. M. Matsuoka for providing nude mice infected with *M. leprae*, and Dr. S. Toratani for peritoneal macrophages. We are also grateful to C. Sakamoto, K. Kawazu, S. Wattanopakayakit, P. D. Bang, and J. Rudeeaneksin for their technical assistance and valuable discussion.

This work was supported by a Grant-in-Aid for Scientific Research on Priority Areas (C) from the Ministry of Education, Culture, Sport, Science and Technology of Japan (No. 13226132 to K.S.), and by a Grant-in-Aid for Research on Emerging and Reemerging Infectious Diseases from The Ministry of Health, Labor, and Welfare of Japan (to M.M.).

VI. References

1. Akira, S. and Takeda, K. (2004) Toll-like receptor signalling. *Nat. Rev. Immunol.* 4; 499–511.
2. Amako, K., Takade, A., Umeda, A., Matsuoka, M., Yoshida, S. and Nakamura, M. (2003) Degradation process of Mycobacterium leprae cells in infected tissue examined by the freeze-substitution method in electron microscopy. *Microbiol. Immunol.* 47; 387–394.
3. Ben-Ali, M., Barbouche, M. R., Bousnina, S., Chabbou, A. and

Dellagi, K. (2004) Toll-like receptor 2 Arg677Trp polymorphism is associated with susceptibility to tuberculosis in Tunisian patients. *Clin. Diagn. Lab. Immunol.* 11; 625–626.
4. Blander, J. M. and Medzhitov, R. (2004) Regulation of phagosome maturation by signals from toll-like receptors. *Science* 304; 1014–1018.
5. Bochud, P. Y., Hawn, T. R. and Aderem, A. (2003) Cutting edge: a Toll-like receptor 2 polymorphism that is associated with lepromatous leprosy is unable to mediate mycobacterial signaling. *J. Immunol.* 170; 3451–3454.
6. de Hostos, E. L., Bradtke, B., Lottspeich, F., Guggenheim, R. and Gerisch, G. (1991) Coronin, an actin binding protein of Dictyostelium discoideum localized to cell surface projections, has sequence similarities to G protein beta subunits. *EMBO J.* 10; 4097–4104.
7. Ferrari, G., Langen, H., Naito, M. and Pieters, J. (1999) A coat protein on phagosomes involved in the intracellular survival of mycobacteria. *Cell* 97; 435–447.
8. Frehel, C. and Rastogi, N. (1987) Mycobacterium leprae surface components intervene in the early phagosome-lysosome fusion inhibition event. *Infect. Immun.* 55; 2916–2921.
9. Fukutomi, Y., Matsuoka, M., Minagawa, F., Toratani, S., McCormick, G. and Krahenbuhl, J. (2004) IL-10 treatment of macrophages bolsters intracellular survival of Mycobacterium leprae. *Int. J. Lepr. Other Mycobact. Dis.* 72; 16–26.
10. Ozinsky, A., Underhill, D. M., Fontenot, J. D., Hajjar, A. M., Smith, K. D., Wilson, C. B., Schroeder, L. and Aderem, A. (2000) The repertoire for pattern recognition of pathogens by the innate immune system is defined by cooperation between toll-like receptors. *Proc. Natl. Acad. Sci. U S A* 97; 13766–13771.
11. Schuller, S., Neefjes, J., Ottenhoff, T., Thole, J. and Young, D. (2001) Coronin is involved in uptake of Mycobacterium bovis BCG in human macrophages but not in phagosome maintenance. *Cell. Microbiol.* 3; 785–793.
12. Suzuki, K., Kobayashi, M. and Kawaoi, A. (1992) Immunohistochemical demonstration of proliferating cell nuclear antigen in growing cells on formalin-fixed, paraffin-embedded tissue sections. *Acta Histochem. Cytochem.* 25; 13–18.
13. Suzuki, K., Nishihata, J., Arai, Y., Honma, N., Yamamoto, K., Irimura, T. and Toyoshima, S. (1995) Molecular cloning of a novel actin-binding protein, p57, with a WD repeat and a leucine zipper motif. *FEBS Lett.* 364; 283–288.
14. Suzuki, K., Lavaroni, S., Mori, A., Ohta, M., Saito, J., Pietrarelli, M., Singer, D. S., Kimura, S., Katoh, R., Kawaoi, A. and Kohn, L. D. (1998) Autoregulation of thyroid-specific gene transcription by thyroglobulin. *Proc. Natl. Acad. Sci. U S A* 95; 8251–8256.
15. Suzuki, K., Lavaroni, S., Mori, A., Okajima, F., Kimura, S., Katoh, R., Kawaoi, A. and Kohn, L. D. (1998) Thyroid transcription factor 1 is calcium modulated and coordinately regulates genes involved in calcium homeostasis in C cells. *Mol. Cell. Biol.* 18; 7410–7422.
16. Suzuki, K., Mori, A., Ishii, K. J., Saito, J., Singer, D. S., Klinman, D. M., Krause, P. R. and Kohn, L. D. (1999) Activation of target-tissue immune-recognition molecules by double-stranded polynucleotides. *Proc. Natl. Acad. Sci. U S A* 96; 2285–2290.
17. Underhill, D. M., Ozinsky, A., Hajjar, A. M., Stevens, A., Wilson, C. B., Bassetti, M. and Aderem, A. (1999) The Toll-like receptor 2 is recruited to macrophage phagosomes and discriminates between pathogens. *Nature* 401; 811–815.
18. Underhill, D. M., Ozinsky, A., Smith, K. D. and Aderem, A. (1999) Toll-like receptor-2 mediates mycobacteria-induced proinflammatory signaling in macrophages. *Proc. Natl. Acad. Sci. U S A* 96; 14459–14463.
19. Zheng, P. Y. and Jones, N. L. (2003) Helicobacter pylori strains expressing the vacuolating cytotoxin interrupt phagosome maturation in macrophages by recruiting and retaining TACO (coronin 1) protein. *Cell. Microbiol.* 5; 25–40.

ANTIMICROBIAL AGENTS AND CHEMOTHERAPY, Apr. 2006, p. 1143–1147 Vol. 50, No. 4
0066-4804/06/$08.00+0 doi:10.1128/AAC.50.4.1143–1147.2006

Organization of Tn*2610* Containing Two Transposition Modules

Akiko Takaya,[1] Masato Watanabe,[2]† and Tomoko Yamamoto[1]*

Department of Microbiology and Molecular Genetics, Graduate School of Pharmaceutical Sciences, Chiba University, Chiba, 263-8522,[1] and Microbiology Laboratories, Institute for Drug Discovery Research, Yamanouchi Pharmaceutical Co., Ltd., Tokyo, 174-8511,[2] Japan

Received 24 March 2005/Returned for modification 15 May 2005/Accepted 5 January 2006

Transposon Tn*2610*, found in a conjugative plasmid from an *Escherichia coli* isolate recovered at a hospital in Chiba, Japan, in 1975, was completely sequenced. Tn*2610* is 23,883 bp long and is bracketed by two transposition modules, a Tn*1721*-like module and a Tn*21*-derived module, which correspond, respectively, to the long inverted repeats IRa and IRb previously described for this transposon. Although both *tnpA* genes are intact, only that in the Tn*21*-derived module (IRb) functions in the transposition, while that in the Tn*1721*-derived module (IRa) cannot recognize the 38-bp imperfect repeat at the end of the IRb element. Both *tnpR* and *res* are present in IRa, while the *tnpR* gene of IRb is interrupted by the insertion of an IS*26* insertion element. The intervening region, between the *res* site of the Tn*1721* module and IS*26*, carries multiple integron-associated resistance genes within a Tn*21* backbone, including a region identical to that found in the genome of *Salmonella enterica* serovar Typhimurium DT104. These findings suggest that Tn*2610* originated from Tn*1721* and Tn*21*, with extensive recombination events with other elements which have resulted in a complex mosaic structure.

Tn*2610* is a multidrug resistance transposon that was originally identified in 1983 on a self-transmissible plasmid, pCS200, originating from an *Escherichia coli* strain isolated in 1975 at a hospital in Chiba, Japan (20). Tn*2610* is 24 kb long and is flanked by 3-kb inverted-repeat (IR) sequences. The intervening nonrepeated region was shown to include genes for resistance to ampicillin, streptomycin, and sulfonamide. Preliminary analysis revealed that Tn*2610* carries two copies of the transposition genes *tnpA* and *tnpR* and that these regions form a stable heteroduplex (19).

Several large transposons conferring resistance to more than one antibiotic have been identified. Among these, Tn*21*, Tn*1691*, Tn*2603*, and Tn*2424*, which are classified as class II transposons, seem to be evolutionarily related (11, 13, 18). On the basis of restriction maps and heteroduplex analyses, we originally proposed that the Tn*21*-related transposons had descended from an ancestral mercury resistance transposon, resembling Tn*2613*, by subsequent insertions of antibiotic resistance genes and/or insertion sequences (18). This hypothesis has been supported by sequence data from a large group of these transposons (11). Current knowledge on Tn*2610* suggests that it may also have evolved from an ancestral mercury resistance transposon via a series of recombination events resulting in a complex configuration.

To confirm this hypothesis, we determined the complete sequence of Tn*2610* and compared its structure to that of other known elements.

* Corresponding author. Mailing address: Department of Microbiology and Molecular Genetics, Graduate School of Pharmaceutical Sciences, Chiba University, Chiba, 263-8522, Japan. Phone: (81) 43-290-2928. Fax: (81) 43-290-2929. E-mail: tomoko-y@p.chiba-u.ac.jp.

† Present address: Astellas Pharma Inc., Tukuba, 300-2698, Japan.

MATERIALS AND METHODS

Bacterial strains and plasmids. The bacterial strains used were *E. coli* DH5α (*supE44 ΔlacU169* [ϕ80 *lacZ* ΔM15] *hsdR17 recA1 endA1 gyrA96 thi-1 relA1*), AB2463 (*recA thr leu thi lac gal ara xyl mtl pro his arg str tsx sup*), and P3478Rif, a rifampin-resistant mutant of P3478 (*thy polA*). The Tn*2610*-containing plasmid used in this study was pTKY170, formerly termed pMK1::Tn*2610*#4 (20). Subcloning for DNA sequencing was performed in pUC18 (17). Plasmids pTKY171 and pTKY172 are pAO3 derivatives carrying Tn*1722* and Tn*1722* with a kanamycin-resistant determinant, respectively. Plasmid pAO3 is a small derivative of plasmid ColE1 (21). Plasmid pTKY173 is a pTKY172 derivative defective in the *tnpA* gene. Plasmids pTKY174 and pTKY175 are pACYC184-based plasmids loaded with *tnpA* genes from Tn*2610* and Tn*1722*, respectively. Bacterial cells were routinely cultured at 37°C in Luria-Bertani (LB) medium or on LB agar. For selection with trimethoprim, Mueller-Hinton agar (Difco Laboratories) was used with 0.5% (vol/vol) lysed horse blood. Antibiotics were added at the following concentrations: ampicillin, 50 μg ml^{-1}; chloramphenicol, 25 μg ml^{-1}; kanamycin, 50 μg ml^{-1}; tetracycline, 25 μg ml^{-1}; trimethoprim, 50 μg ml^{-1}; rifampin, 100 μg ml^{-1}.

Construction of plasmids. Plasmid pTKY171 (pAO3::Tn*1722*) was derived from plasmid pAO3::Tn*1721* by deletion of the DNA fragment between the SalI site at nucleotide (nt) 6946 in Tn*1721* (Fig. 1) and the BstEII site in pAO3. The pUC4K-derived kanamycin resistance determinant was inserted into the AvaI site at nt 991 in Tn*1722* (Fig. 1), resulting in pTKY172. Plasmid pTKY173 is an AvaI-generated deletion of pTKY172 which was cleaved at nt 2855 and nt 4562 in Tn*1722* and self-ligated. The DNA fragment between the EcoRI site at nt 13 and the BamHI site at nt 4157 in Tn*2610* from pTKY170 was cloned into BamHI-digested pACYC184, resulting in pTKY174. Plasmid pTKY175 was constructed by cloning of the DNA fragment between nt 13 and nt 5624 in Tn*1722* into EcoRI-digested pACYC184.

Determination of transposition proficiency. The mating-out assay was used to determine transposition frequency (19). The pACYC184-based plasmid loaded with a relevant *tnpA* gene was introduced into AB2463 containing R388, a conjugative plasmid devoid of transposable elements, and pTKY173. The resulting strain was used as a donor to mate with the recipient strain P3478Rif. Donor and recipient strains were mixed in a 1:5 ratio and passed through a Millipore filter, and then the filters were incubated on the agar plates at 37°C for 6 h. Transconjugants receiving R388::Tn*1722* were selected with kanamycin and rifampin. Transconjugants receiving R388 were selected with trimethoprim and rifampin. The transposition frequency was expressed as the ratio of the number of kanamycin-resistant transconjugants to the number of R388 transconjugants.

DNA isolation and restriction mapping. Plasmid DNA for restriction analysis and cloning was isolated by the alkaline lysis method (3). Restriction enzymes (TaKaRa Bio Inc., TOYOBO) were used in accordance with the manufacturer's

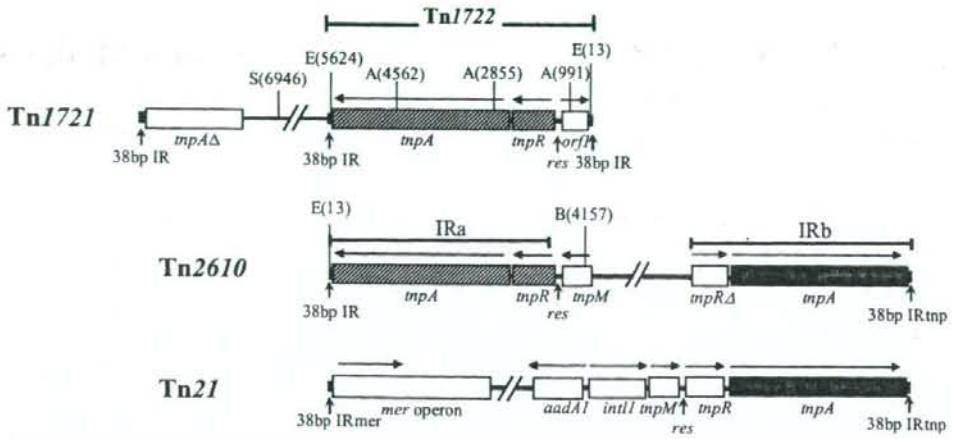

FIG. 1. Structure of the transposition modules forming the backbone of Tn*2610*. Arrows above open bars indicate the transcription orientations of the ORFs. Restriction cleavage sites shown are those used for the construction of plasmid derivatives described in Materials and Methods. The structures and restriction sites are based on GenBank sequences for Tn*2610* (accession no. AB207867) and Tn*1721* (X61367). Abbreviations: A, AvaI; B, BamHI; E, EcoRI; S, SalI.

TABLE 1. Features of ORFs and discrete DNA segments in Tn*2610*

Location[a] (5'–3')	DNA segment	ORF[b] No.	ORF[b] Name	ORF[b] Size[c]	% Homology (DNA/aa)	Description of gene or gene product (accession no.)
1–38	IR					38-bp IR in 1Ra of Tn*2610*
34–3000		S01	*tnpA*	988	99.7/99.2	Transposase from Tn*1721* (X61367)
3004–3564		S02	*tnpR*	186	99.8/100	Resolvase from Tn*1721* (X61367)
3627–3755	*res*					*resIII* (3627–3656), *resII* (3661–3703), *resI* (3717–3755)
3740–4324		S03	*tnpM*	194	100/100	TnpM on Tn*21* (AF071413)
4091–5376	5'-CS					Partial 5'-CS of class 1 integron (AF261825)
4091–4114	IRi					IRi of class 1 integron (AF261825)
4293–5306		S04	*intI1*	337	100/100	Integrase of class 1 integron (AY214164)
5873–6079		S05	small ORF	68	100/100	Small ORF from pIP1527 (X03988)
6079–7338		S06	*ereB*	419	100/100	Erythromycin esterase type II (X03988)
7661–9145		S07	orf2	494	100/100	Putative OrfA from SGI1 (AF261825)
9420–10073		S08	*groEL/intI1*	217	100/100	GroEl/integrase fusion protein from SGI1
9777–10209	5'-CS					Partial 5'-CS of class 1 integron (AF261825)
10154–10209	*attI*					*attI* of class 1 integron (AF261825)
10279–11145		S09	*pse-1*	288	100/100	PSE-1 β-lactamase from SGI (AF261825)
11275–12054		S10	*aadA2*	259	100/100	Streptomycin resistance protein (AF164956)
12056–12114	59 bp					59-bp element of class 1 integron (AF261825)
12114–14134	3'-CS					3'-CS of class 1 integron (AF261825)
12218–12565		S11	*qacEΔ1*			Quaternary ammonium compound and disinfectant resistance partial protein on SGI
12559–13398		S12	*sul1*	279	100/100	Sulfonamide resistance protein on SGI
13526–14026		S13	*orf5*	166	100/100	Putative acetyltransferase in Tn*21* (AF071413)
14050–14134		S14	*orf6Δ*			Hypothetical partial protein (AF261825)
14135–14160	IR					Terminal IR of IS*1326* (AY123253.3)
14202–14987		S15	*istB*	261	100/100	Unknown function of IS*1326* (AY123253.3)
14974–16497		S16	*istA*	507	100/100	Possible transposase of IS*1326* (AY123253.3)
16579–16590	IR					Terminal IR of IS*1353* (AY123523)
16620–18164		S17	OrfAB	516	100/100	OrfAB from IS*1353* (AY123523)
18180–18192	IR					Terminal IR of IS*1353* (AY123253.3)
18195–18280	IR					Terminal IR of IS*1326* (AY123253.3)
18215–19075		S18	*tniBΔ1*			Truncated TniB from In2 (U42226)
19078–19512		S19	*tniA*			Partial TniA of In2 (U42226)
19513–19527	IR					IR of IS*26* (AY123523)
19575–20282		S20	*tnpA*	235	100/100	Transposase of IS*26* (AY123523)
20321–20333	IR					IR of IS*26* (AY123523)
20334–20881		S21	*tnpR*			Truncated resolvase of Tn*21* (AF071413)
20884–23850		S22	*tnpA*	988	100/100	Transposase of Tn*21* (AF071413)
23846–23883	IR					38-bp IR in IRb of Tn*2610*

[a] Nucleotide position in the sequence deposited under accession no. AB207867.
[b] Named ORFs are based on those previously characterized.
[c] Expressed as the number of amino acid residues.

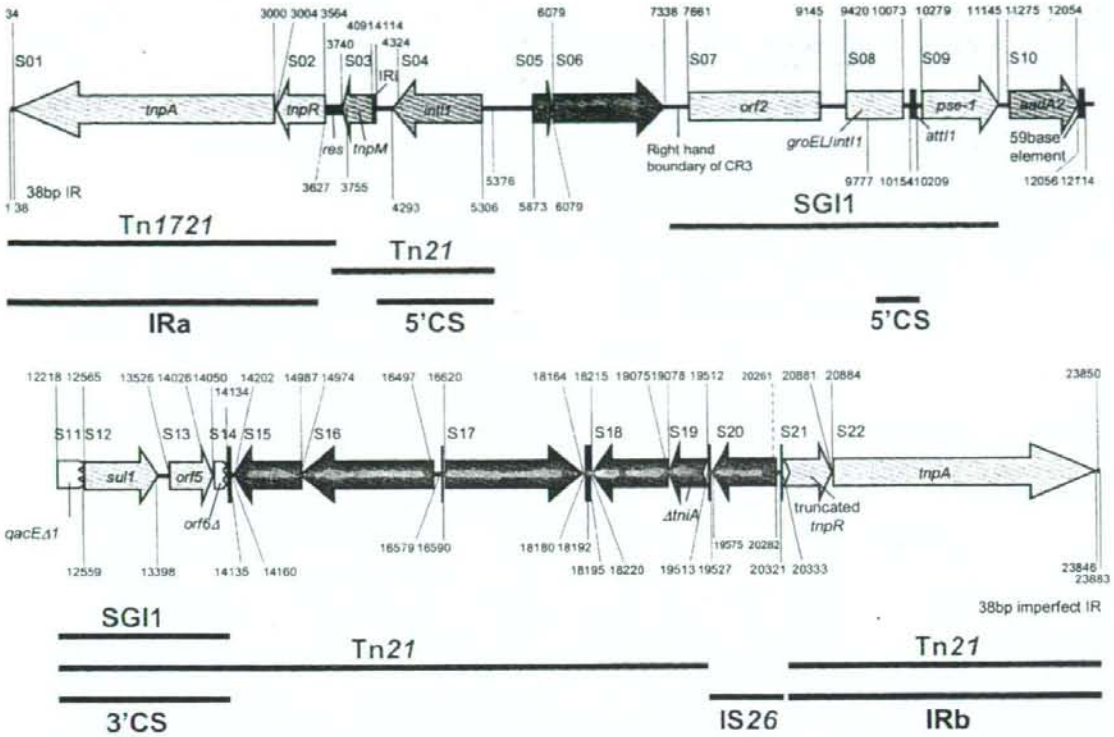

FIG. 2. Genetic organization of Tn*2610* based on complete nucleotide sequence analysis. Labeled lines represent the regions in which sequences exhibit significant homology to extant sequences on various genetic elements. The accession numbers of the sequences used for comparative analysis are given in Table 1.

instructions. DNA fragments were separated by electrophoresis on 1% (wt/vol) agarose gels, and individual fragments were isolated from the gels using a QIAEX II gel extraction kit (QIAGEN). HindIII-digested lambda phage DNA fragments and HinfII-digested pBR322 plasmid DNA fragments were used as size markers.

Sequence analysis. Sequencing was performed in the facility at QIAGEN, Japan, on an ABI PRISM model 3100 sequencer. DNA sequences were assembled using the GENETYX version 10.1 software package. PCR was used to amplify the pTKY170 fragments to confirm the boundaries between the cloned fragments predicted by mapping and to obtain sequences. The sequence obtained was used to query the GenBank database in order to identify putative genes by using the BLAST program via the World Wide Web interface of the National Center for Biotechnology Information (http://www.ncbi.nlm.nih/BLAST).

Nucleotide sequence accession number. The 23,883-bp sequence of Tn*2610* has been submitted to the DDBJ/EMBL/GenBank databases under accession no. AB207867.

RESULTS AND DISCUSSION

General features of the Tn*2610* sequence. To complete the sequence of Tn*2610*, plasmid pTKY170 (formerly named pMK1::Tn*2610*#4 [20]), containing a complete copy of the transposon, was initially subjected to restriction analysis, and relevant fragments were subcloned for sequencing. The complete sequence of the 23,883-bp region bracketed by the previously characterized inverted repeats IRa (formerly named IR-R) and IRb (formerly named IR-L), which are defined by 5-bp direct repeats at their outer ends, was determined. A total of 22 open reading frames (ORFs) were identified and are listed in Table 1. The putative products encoded by these ORFs either were identical to or exhibited significant homology to protein sequences available in GenBank. The nature and positions of relevant features (even in the noncoding regions) are also shown in Table 1. Figure 2 is a linear map of Tn*2610* showing the transposon structure.

Tn*2610* contains two modules for transposition. Analysis of the sequence showed that Tn*2610* is composed of two transposition modules, a Tn*1721*-like module and a Tn*21*-derived module, which correspond, respectively, to IRa and IRb (Fig. 2). Within the Tn*1721*-like (IRa) module, the transposase gene *tnpA*, the resolvase gene *tnpR*, and the *res* site show strong homology to the corresponding regions of Tn*1721* (Table 1; Fig. 2 and 3) (1). A 38-bp sequence was identified at one end of IRa, differing in 3 bases from that in Tn*1721* (Fig. 3A). The 129-bp *res* site of IRa is identical to that of Tn*1721* as far as *resI*, where recombination has occurred with the *res* site of Tn*21* (Fig. 3B) (16).

In contrast, IRb is a Tn*21* remnant including a partially deleted *tnpR* gene, *tnpA*, and a 38-bp IR identical to those in

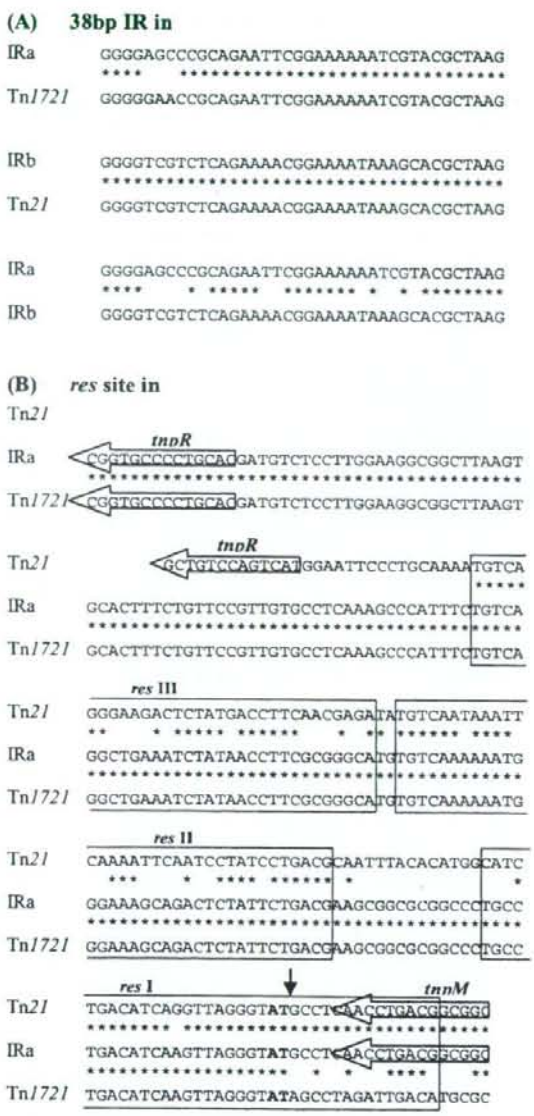

FIG. 3. Comparison of the 38-bp inverted repeats (A) and *res* sites (B). The sequences of the 38-bp inverted repeats and *res* sites in Tn*2610* IRa (this study), Tn*1721* (accession no. X61367), and Tn*21* (accession no. AF071413) are aligned, with asterisks indicating identical bases. The *res* subsites (9) are boxed, and the AT site at which resolvase-mediated recombination takes place is boldfaced. The recombination crossover point to generate the hybrid *res* is indicated by a vertical arrow. *tnpR* and *tnpM*, regions adjacent to each end of the *res* sites.

Tn*21* (Fig. 2). The *tnpR* gene is interrupted by the insertion of an IS*26* insertion element, leading to the loss of 12 bp including the ATG start codon of the gene and the *res* site. Taking all these findings together, we conclude that Tn*2610* is bracketed by 38-bp imperfect IRs (10-bp differences) (Fig. 3) at both ends and carries two intact *tnpA* genes, one intact *tnpR* gene, and one *res* site as a transposition module.

TABLE 2. Complementation of a Tn*1722*Δ*tnpA* mutant

Complementing plasmid (*tnpA*)	Transposition frequency[a]
pTKY175 (Tn*1722*)	2.3×10^{-2}
pTKY174 (Tn*2610* IRa)	3.0×10^{-2}
pACYC184	$<10^{-4}$

[a] Determined as described in Materials and Methods.

Our earlier analysis indicated that *tnpA* in IRb is functional, while *tnpA* in IRa is not functional, in the transposition of Tn*2610* (19). Although the IRa module shows strong homology to that of Tn*1721*, the corresponding genes are not identical. The *tnpA* gene in IRa differs from the Tn*1721* sequence at nine positions, leading to the alteration of 7 amino acid residues. Furthermore, a 3-base difference is found in the 38-bp IR sequences between IRa and Tn*1721* (Fig. 3A). Therefore, the inability of *tnpA* in IRa to promote the transposition of Tn*2610* may be due to a mutation. To determine whether the *tnpA* gene of IRa is active, the ability of the product to promote the transposition of Tn*1721* was examined by complementation analysis of a Tn*1722 tnpA*-defective mutant as described in Materials and Methods. As shown in Table 2, the *tnpA* gene in IRa complemented the *tnpA* defect in Tn*1722*, suggesting that it is active even though it cannot promote the transposition of Tn*2610*. The Tn*1721*-like *tnpA* product of IRa probably cannot recognize the 38-bp element at the end of IRb, while the Tn*21*-like *tnpA* product of IRb recognizes both 38-bp elements, even though they are imperfect. This hypothesis is supported by a report showing that the Tn*21 tnpA* products can act on the IR of Tn*501* (which is identical to the IR of Tn*1721*) but the Tn*501 tnpA* product cannot promote the transposition of Tn*21* (8).

The intervening nonrepeated region of Tn*2610*. Analysis of the intervening nonrepeated region from nt 3514 to nt 20333 reveals the presence of discrete DNA regions carried between the two transposition modules in Tn*2610* (Fig. 2).

The Tn*1721*-like transposition module merges (at the *res* site) with a Tn*21*-derived sequence (nt 3565 to 5376) including *tnpM* and the 5′ conserved segment (5′-CS) of the class 1 integron (the insertion site of the integron IRi into *tnpM* is identical to that in Tn*21*). The *intI1* gene, in this case, is not preceded by an *attI1* site (14) with inserted gene cassettes but by a segment containing the *ereB* gene (2) with part of CR3 (15). The right-hand boundary of CR3 merges with a long region (nt 7339 to 14134) identical to a part of *Salmonella* genomic island I (SGI1) (5) of *Salmonella enterica* serovar Typhimurium phage type DT104 except for the presence of an additional *aadA2* cassette in Tn*2610*. This region includes *orf2* (5, 11), the remnant of the 5′-CS of a class 1 integron containing an *intI1-groEL* hybrid, two gene cassettes (bla_{PSE-1} and *aadA2*), and the 3′-CS of a class 1 integron including *qacEΔ1*, *sul1*, *orf5*, and *orf6*Δ (Fig. 2), which is also identical to that found in In2 carried on Tn*21* (11, 15). The homology with In2 continues down to the *tniA* gene, which is interrupted by the

IS*26* insertion element (at nt 20333) located between this region and IRb (Fig. 2).

This complex mosaic structure is likely derived by multiple recombination events which involved Tn*21*-like and SGI1-like sequences, as well as other sequences.

Concluding remarks. The present study has shown that Tn*2610* is a composite transposon comprising two transposition modules, Tn*1721*-like IRa and Tn*21*-derived IRb, surrounding a central region containing the drug resistance genes *ereB*, *pse-1*, *aadA2*, and *sul1*. It is proposed that the ancestors of Tn*1721* and Tn*21* were independently inserted into a plasmid or genome via transposition events catalyzed by their own transposition modules, leading to the backbone of Tn*2610*. Later, genes could have been lost by deletion during or after the acquisition of the regions that include the integrons. This seems plausible, since a transposon carrying *mphB* with an organization very similar to that of the transposition modules in Tn*2610* has been found in *E. coli* (12).

SGI1 has been identified in DT104, whose prevalence increased dramatically in the 1990s (4, 5, 7, 10). DT104 isolates have been reported to be resistant to a core group of antibiotics including ampicillin, chloramphenicol, streptomycin, sulfonamide, and tetracycline (commonly abbreviated ACSSuT). Furthermore, a number of variants of SGI1 that are associated with different resistance phenotypes (e.g., ACSSuS plus trimethoprim, SSu, ASu, and ASSuT) have been identified, suggesting that the multidrug resistance region of SGI1 was subject to recombination events that generated variants (4, 6). Since Tn*2610* was found in a plasmid from a strain isolated before SGI1-containing strains, it could also have been involved in the generation of SGI1 structures.

ACKNOWLEDGMENTS

We thank T. Tomoyasu and N. Kon for technical assistance.

This work was supported in part by a grant from the Research Project for Emerging and Reemerging Infectious Diseases (H15-Shinkou-9) from the Ministry of Health, Labor and Welfare of Japan.

REFERENCES

1. **Allmeier, H., B. Cresnar, M. Greck, and R. Schmitt.** 1992. Complete nucleotide sequence of Tn*1721*: gene organization and a novel gene product with features of a chemotaxis protein. Gene **111**:11–20.
2. **Arthur, M., D. Autissier, and P. Courvalin.** 1986. Analysis of the nucleotide sequence of the *ereB* gene encoding the erythromycin esterase type II. Nucleic Acids Res. **14**:4987–4999.
3. **Birnboim, H. C., and J. Doly.** 1979. A rapid alkaline extraction procedure for screening recombinant plasmid DNA. Nucleic Acids Res. **7**:1513–1523.
4. **Boyd, D., A. Cloeckaert, E. Chaslus-Dancla, and M. R. Mulvey.** 2002. Characterization of variant *Salmonella* genomic island 1 multidrug resistance regions from serovars Typhimurium DT104 and Agona. Antimicrob. Agents Chemother. **46**:1714–1722.
5. **Boyd, D. A., G. A. Peters, A. Cloeckaert, K. S. Boumedine, E. Chaslus-Dancla, H. Imberechts, and M. R. Mulvey.** 2001. Complete nucleotide sequence of a 43-kilobase genomic island associated with the multidrug resistance region of *Salmonella enterica* serovar Typhimurium DT104 and its identification in phage type DT120 and serovar Agona. J. Bacteriol. **183**: 5725–5732.
6. **Doublet, B., D. Boyd, M. R. Mulvey, and A. Cloeckaert.** 2005. The *Salmonella* genomic island 1 is an integrative mobilizable element. Mol. Microbiol. **55**:1911–1924.
7. **Glynn, M. K., C. Bopp, W. Dewitt, P. Dabney, M. Mokhtar, and F. J. Angulo.** 1998. Emergence of multidrug-resistant *Salmonella enterica* serotype Typhimurium DT104 infections in the United States. N. Engl. J. Med. **338**: 1333–1338.
8. **Grinsted, J., F. de la Cruz, and R. Schmitt.** 1990. The Tn*21* subgroup of bacterial transposable elements. Plasmid **24**:163–189.
9. **Hall, S. C., and S. E. Halford.** 1993. Specificity of DNA recognition in the nucleoprotein complex for site-specific recombination by Tn*21* resolvase. Nucleic Acids Res. **21**:5712–5719.
10. **Izumiya, H., J. Terajima, S. Matsushita, K. Tanuma, and H. Watanabe.** 2001. Characterization of multidrug-resistant *Salmonella enterica* serovar Typhimuirum isolated in Japan. J. Clin. Microbiol. **39**:2700–2703.
11. **Liebert, C. A., R. M. Hall, and A. O. Summers.** 1999. Transposon Tn*21*, flagship of the floating genome. Microbiol. Mol. Biol. Rev. **63**:507–522.
12. **Noguchi, N., J. Katayama, and M. Sasatsu.** 2000. A transposon carrying the gene *mphB* for macrolide 2′-phosphotransferase II. FEMS Microbiol. Lett. **192**:175–178.
13. **Ouellette, M., L. Bissonnette, and P. H. Roy.** 1987. Precise insertion of antibiotic resistance determinants into Tn*21*-like transposons: nucleotide sequence of the OXA-1 β-lactamase gene. Proc. Natl. Acad. Sci. USA **84**:7378–7382.
14. **Partridge, S. R., G. D. Recchia, C. Scaramuzzi, C. M. Collis, H. W. Stokes, and R. M. Hall.** 2000. Definition of the *attI1* site of class 1 integrons. Microbiology **146**:2855–2864.
15. **Partridge, S. R., H. J. Brown, H. W. Stokes, and R. M. Hall.** 2001. Transposons Tn*1696* and Tn*21* and their integrons In4 and In2 have independent origins. Antimicrob. Agents Chemother. **45**:1263–1270.
16. **Rogowsky, P., S. E. Halford, and R. Schmitt.** 1985. Definition of three resolvase binding sites at the *res* loci of Tn*21* and Tn*1721*. EMBO J. **4**:2135–2141.
17. **Sambrook, J., E. F. Fritsch, and T. Maniatis.** 1989. Molecular cloning: a laboratory manual, 2nd ed. Cold Spring Harbor Laboratory, Cold Spring Harbor, N.Y.
18. **Tanaka, M., T. Yamamoto, and T. Sawai.** 1983. Evolution of complex resistance transposons from an ancestral mercury transposon. J. Bacteriol. **153**: 1432–1438.
19. **Yamamoto, T.** 1989. Organization of complex transposon Tn*2610* carrying two copies of *tnpA* and *tnpR*. Antimicrob. Agents Chemother. **33**:746–750.
20. **Yamamoto, T., M. Watanabe, K. Matsumoto, and T. Sawai.** 1983. Tn*2610*, a transposon involved in the spread of the carbenicillin-hydrolysing β-lactamase gene. Mol. Gen. Genet. **189**:282–288.
21. **Yamamoto, T., S. Yamagata, Y. Hashimoto, and S. Yamagishi.** 1980. Restriction endonuclease cleavage maps of the ampicillin transposons Tn*2601* and Tn*2602*. Microbiol. Immunol. **24**:1139–1149.

IV. 資料

特許公開のお知らせ

整理番号　：　006C1003
発明の名称　：　ペニシリン耐性B群連鎖球菌(Group B streptococcus)を識別する方法及び識別用キット
発明機関名　：　国立感染症研究所
出願日 番号　：　2006. 7. 11　特願2006－190059
公開日 番号　：　2008. 1. 31　特開 2008－017723
発明者　：　(細菌第二部)；木村 幸司、 黒川 博史、 荒川 宜親
発明の概要　：

ペニシリン耐性B群連鎖球菌(Group B streptococcus)を簡便に識別できる方法及びキットを提供する。

検出対象である菌が塗布された固体培地の表面に、オキサシリン、セフチゾキシム、またはセフチブテン(薬剤)を点在させ、上記固体培地を培養し、培養後、上記薬剤の周囲に形成される阻止円の大きさの基準値との違いにより、検出対象である菌がペニシリン耐性B群連鎖球菌であるか否かを識別する方法。ストリップ状の基体にオキサシリン、セフチゾキシム、およびセフチブテンを、距離を置いて配置したペニシリン耐性B群連鎖球菌識別用キット。

オキサシリン、セフチゾキシム、またはセフチブテンを段階的に希釈して含有する複数の液体培地を用意し、各液体培地に、検出対象である菌を接種し、培養を行い、培養後、最小阻止濃度(MIC)の低下の有無および／または程度から、検出対象である菌がペニシリン耐性B群連鎖球菌であるか否かを識別する方法。

病院での検査に有用である。

詳細情報を希望される方は、「出願明細書送付依頼」に必要事項をご記入の上、HSTTC宛にお送りください。

特許公開のお知らせ

整理番号　：　006C1002
発明の名称　：　新規キノロン系抗菌薬排出ポンプ
発明機関名　：　国立感染症研究所
出願日 番号　：　2006. 7. 7　　特願2006－187660
公開日 番号　：　2008. 1. 24　　特開2008－011805
発明者　：　(細菌第二部)；山根　一和、　荒川　宜親
発明の概要　：

新規のキノロン系抗菌薬耐性大腸菌、E. coli C316 株の、キノロン系抗菌薬耐性の原因を明らかにすることを課題とする。本発明はまた、その様なキノロン系抗菌薬耐性を有する細菌を特定する手段を開発することを課題とする。

細菌の細胞内からキノロン系抗菌薬を排出する活性を有するタンパク質およびこのタンパク質をコードする塩基配列を有する核酸を提供する。本発明はさらに、被検細菌サンプルに対してPCR反応またはまたはサザンブロットハイブリダイゼーション法を行って、qep 遺伝子 SEQ ID NO: 1)の存在の有無を検出することによる、細胞内からキノロン系抗菌薬を排出する活性を有する細菌の検出方法もまた提供する。

医療現場において、qep 遺伝子によりもたらされるキノロン系抗菌薬に対する耐性の臨床診断が可能になる。

詳細情報を希望される方は、「出願明細書送付依頼」に必要事項をご記入の上、HSTTC宛にお送りください。

特許公開のお知らせ

整理番号　：　006C1005
発明の名称　：　新規な16S rRNAメチラーゼ遺伝子、該遺伝子から産生されるタンパク質、および、それらの検査方法
発明機関名　：　国立感染症研究所
出願日 番号　：　2006. 9. 11　　特願2006－245775
公開日 番号　：　2008. 3. 21　　特開2008－061625
発明者　：　(細菌第二部)；荒川 宜親、　和知野 純一
発明の概要　：

新規な耐性機構を付与する16S rRNAメチラーゼ遺伝子、その検査方法、その検査に使用するプライマー、該プライマーを用いた検査キット プローブ、該プローブを用いた検査薬、並びに、前記遺伝子から産生されるタンパク質、該タンパク質を用いる該タンパク質を検出するための検査方法、該タンパク質に対する抗体、および該抗体を含有する検査薬を提供する。

配列番号 1の塩基配列から成ることを特徴とする遺伝子、および該遺伝子から産生された配列番号 2のアミノ酸配列からなるタンパク質。

既出願(特願 2005-255755)のものとは遺伝子が違う。　遺伝子が医療機関や臨床検査センター等における日常の細菌検査業務の中で、アミノ配糖体耐性遺伝子を保有する菌を速やかに識別し除去することが可能となる。

詳細情報を希望される方は、「出願明細書送付依頼」に必要事項をご記入の上、HSTTC宛にお送りください。

特許出願のお知らせ

整理番号	:	005C1003
発明の名称	:	新規な16S rRNAメチラーゼ遺伝子、該遺伝子から産生されるタンパク質、および、それらを用いた該遺伝子またはそれによって産生された16S rRNA メチラーゼの検出方法
発明機関名	:	国立感染症研究所
出願日 番号	:	2005. 9. 2　　特願2005－255755
国際出願日 番号	:	2006. 9. 4　　PCT/JP2006／317439
国際公開日 番号	:	2007. 3. 8　　WO 2007／026926
発明者	:	(細菌第二部)；荒川 宜親、　　和知野 純一
発明の概要	:	

広範囲のアミノ配糖体抗生物質に対して高度耐性を獲得した腸内細菌の新規な耐性機構を付与する16S rRNA メチラーゼ、およびそれを産生している遺伝子の情報を提供する。
配列番号 1の塩基配列から成ることを特徴とする遺伝子、および該遺伝子から産生された配列番号 2のアミノ酸配列からなるタンパク質。

医療機関や臨床検査センター等における日常の細菌検査業務の中で、アミノ配糖体耐性遺伝子を保有する菌を速やかに識別し除去することが可能となる。

詳細情報を希望される方は、「出願明細書送付依頼」に必要事項をご記入の上、HSTTC宛にお送りください。

Serodiagnosis of *Mycobacterium avium*–Complex Pulmonary Disease Using an Enzyme Immunoassay Kit

Seigo Kitada[1], Kazuo Kobayashi[2], Satoshi Ichiyama[3], Shunji Takakura[3], Mitsunori Sakatani[4], Katsuhiro Suzuki[4], Tetsuya Takashima[5], Takayuki Nagai[5], Ikunosuke Sakurabayashi[6], Masami Ito[7], Ryoji Maekura[1], for the MAC Serodiagnosis Study Group

[1]Department of Internal Medicine, National Hospital Organization (NHO) National Toneyama Hospital, Toyonaka-shi, Osaka, Japan; [2]Department of Immunology, National Institute of Infectious Diseases, Shinjuku-ku, Tokyo, Japan; [3]Department of Clinical Laboratory Medicine, Graduate School of Medicine, Kyoto University, Kyoto-shi, Kyoto, Japan; [4]Department of Internal Medicine, NHO Kinki-chuo Chest Medical Center, Sakai-shi, Osaka, Japan; [5]Department of Medicine, Osaka Prefectural Medical Center for Respiratory and Allergic Diseases, Habikino-shi, Osaka, Japan; [6]Department of Laboratory Medicine, Saitama Medical Center, Jichi Medical University, Saitama-shi, Saitama, Japan; and [7]Department of Internal Medicine, Sakamoto Hospital, Toyonaka-shi, Osaka, Japan

Rationale: The diagnosis of *Mycobacterium avium*–complex pulmonary disease (MAC-PD) and/or its discrimination from pulmonary tuberculosis (TB) is sometimes complicated and time consuming.

Objectives: We investigated in a six-institution multicenter study whether a serologic test based on an enzyme immunoassay (EIA) kit was useful for diagnosing MAC-PD and for distinguishing it from other lung diseases.

Methods: An EIA kit detecting serum IgA antibody to glycopeptidolipid core antigen specific for MAC was developed. Antibody levels were measured in sera from 70 patients with MAC-PD, 18 with MAC contamination, 37 with pulmonary TB, 45 with other lung diseases, and 76 healthy subjects.

Measurements and Main Results: Significantly higher serum IgA antibody levels were detected in patients with MAC-PD than in the other groups ($P < 0.0001$). Setting the cutoff point at 0.7 U/ml resulted in a sensitivity and specificity of the kit for diagnosing MAC-PD of 84.3 and 100%, respectively. Significantly higher antibody levels were also found in patients with nodular-bronchiectatic disease compared with fibrocavitary disease in MAC-PD ($P < 0.05$). There was a positive correlation between the extent of disease on chest computed tomography scans and the levels of antibody ($r = 0.43$, $P < 0.05$) in patients with MAC-PD.

Conclusions: The EIA kit is useful for the rapid diagnosis of MAC-PD and for differentiating MAC-PD from pulmonary TB and, if validated by studies in other populations, could find wide application in clinical practice.

Keywords: nontuberculous mycobacteria; immunocompetence; sensitivity and specificity

AT A GLANCE COMMENTARY

Scientific Knowledge on the Subject

The diagnosis of pulmonary disease due to ubiquitous *Mycobacterium avium* complex (MAC) is complicated, and requires clinical findings together with repeatedly positive sputum culture.

What This Study Adds to the Field

An enzyme immunoassay kit for measuring human serum antibody to glycopeptidolipid core antigen specific for MAC was developed. The kit is useful for the serodiagnosis of MAC pulmonary disease and could find wide application in clinical practice.

The prevalence of disease due to nontuberculous mycobacteria has been increasing recently (1–5). In Japan, *Mycobacterium avium* complex (MAC) accounts for approximately 70% of nontuberculous mycobacterial disease (6). MAC is now widely recognized as an important pathogen that causes chronic and progressive pulmonary disease even in immunocompetent patients and not only in those who are immunosuppressed. The diagnosis of MAC-PD is complicated because, in contrast to *Mycobacterium tuberculosis*, MAC contamination of clinical specimens can come from environmental sources such as water, dust, and soil, and because this organism may colonize the respiratory tract without any accompanying invasive disease (4). Thus, isolation of MAC from sputa is often of no clinical significance. Diagnosis of pulmonary disease due to MAC is complicated and time consuming when made according to the guidelines of the American Thoracic Society (ATS) (1), because MAC is ubiquitous in nature and the diagnosis requires clinical findings and its repeated isolation from sputum. In addition, it is also difficult to discriminate MAC-PD from infection due to other mycobacteria in the absence of culture results, because clinical features, such as symptomatic or radiographic findings, are very similar in mycobacterial diseases. In the context of infection control, it is particularly important to distinguish between MAC-PD and pulmonary tuberculosis (TB).

To overcome these difficulties, we have developed a serologic test for the glycopeptidolipid (GPL) antigen specific for MAC, and have reported its clinical usefulness (7–9). The levels of antibody to GPL core were measured by an enzyme immunoassay (EIA) using sera of immunocompetent patients with MAC-PD. MAC-PD could be discriminated from pulmonary TB, *Mycobacterium kansasii* pulmonary disease and MAC colonization/contamination using this serologic test. Healthy subjects were seronegative. Of the different immunoglobulin (Ig) subclasses, best results were obtained by the measurement of IgA, with a sensitivity of 92.5% and specificity of 95.1%. These results suggest that the test is useful as a diagnostic aid. In the present study, to apply this test widely in clinical practice, we

(*Received in original form May 25, 2007; accepted in final form December 13, 2007*)

Supported by grants from the Ministry of Health, Labor, and Welfare (Research on Emerging and Re-emerging Infectious Diseases, Health Sciences research grants); the Ministry of Education, Culture, Sports, Science, and Technology; Tauns Laboratory, Inc.; and the Osaka Tuberculosis Research Foundation.

Correspondence and requests for reprints should be addressed to Seigo Kitada, M.D., Department of Internal Medicine, National Hospital Organization National Toneyama Hospital, 5-1-1 Toneyama, Toyonaka-shi, Osaka 560-8552, Japan. E-mail: kitadas@toneyama.hosp.go.jp

This article contains an online supplement, which is accessible from this issue's table of contents at www.atsjournals.org

Am J Respir Crit Care Med Vol 177. pp 793–797, 2008
Originally Published in Press as DOI: 10.1164/rccm.200705-771OC on December 13, 2007
Internet address: www.atsjournals.org

developed an EIA kit detecting serum IgA antibody specific for GPL core and investigated its usefulness in a multicenter study.

METHODS

See the online supplement for additional methodologic details.

Patients and Serum Samples

Six institutions participated in this study. Between June 2003 and December 2005, serum samples were collected from 70 patients with MAC-PD, 18 with MAC contamination, 36 with pulmonary TB, 45 with other lung diseases, and 76 healthy subjects. All patients with MAC-PD met the ATS guidelines (1). Of the 70 patients with MAC-PD, 64 had previously received combination chemotherapy for mycobacterial diseases recommended by the ATS guidelines, but had MAC-positive cultures at the time of serum collection. Pulmonary TB was confirmed by culture positivity for *M. tuberculosis*. Patients with pulmonary TB who had an underlying pulmonary disease or past history of treatment for pulmonary TB were excluded. Individuals with MAC contamination showed a single culture positive for MAC in small amounts, but were asymptomatic and had no significant chest computed tomography (CCT) findings indicating active mycobacterial disease. The other lung diseases included chronic obstructive pulmonary disease (n = 15), idiopathic interstitial pneumonia (n = 11), lung cancer (n = 11), bacterial pneumonia (n = 4), pulmonary sarcoidosis (n = 2), and bronchiectasis (n = 2). All sera were stored at −20°C until assayed for IgA GPL core antibody. None of the patients was seropositive for HIV type 1 or 2. The patients with MAC-PD were classified into two groups on the basis of the chest radiography: fibrocavitary disease and nodular-bronchiectatic (NBE) disease (1).

Fibrocavitary disease was defined as the presence of cavitary forms in upper lobes. NBE disease was defined as the presence of bronchiectasis and multiple nodular shadows on CCT. Disease conforming to neither of these types was considered unclassifiable. Forty-five patients underwent CCT and serodiagnosis at the same time. A correlation between the extent of disease and antibody levels was investigated. The extent of disease was expressed as the number of MAC-involved CCT segments, as described in the previous study (9).

The studies in human subjects were approved by the research and ethical committees of the NHO National Toneyama Hospital, and written, informed consent was obtained from all subjects.

EIA Kit

The EIA kit was developed by Tauns Laboratories, Inc. (Shizuoka, Japan), with a slight modification of the method described previously (8). Results are given as arbitrary U/ml in relation to a standard curve that was constructed by mixing sera from three patients with MAC-PD as a reference. The intra- and interplate coefficients of variation were 2.27–9.29% and 0.57–8.86%, respectively, which indicated good reproducibility. The linearity of measurement was confirmed. The influence of blood elements and temperature was examined, and revealed good stability. The assay was performed by a technologist with no prior knowledge of the clinical data.

Statistical Analysis

All statistical analyses were performed using GraphPad Prism version 4 (GraphPad Software, Inc., San Diego, CA). Antibody levels in patient groups are expressed as means ± SD. For comparison of the mean values of multiple groups, data were compared by analysis of variance and nonparametric analysis. A probability value of less than 0.05 was regarded as significant.

RESULTS

Study Subjects

The characteristics of the subjects are shown in Table 1. Patients with pulmonary TB and healthy subjects were younger than patients with MAC-PD ($P < 0.001$), and there was a larger proportion of females in the latter group ($P < 0.001$). Of the 70 patients with MAC-PD, 15 had underlying pulmonary disease, all of which were the sequelae of pulmonary TB. Of the 18 individuals with MAC contamination, 15 had underlying pulmonary diseases (8 patients with the sequelae of pulmonary TB, 2 with lung cancer, 2 with chronic obstructive pulmonary disease, 1 with emphysema, 1 with pneumoconiosis, and 1 with sarcoidosis. Of the patients with MAC-PD, 19 were classified as having fibrocavitary disease, and 35 as having NBE disease, with 16 patients unclassifiable. The MAC-PD group included infections with *M. avium* (n = 56), *Mycobacterium intracellulare* (n = 12), or both (n = 2). The MAC contamination group included *M. avium* (n = 16) and *M. intracellulare* (n = 2).

Level of GPL Core IgA Antibody

The level of serum IgA antibody to GPL core was quantified using the EIA kit (Figure 1). As expected, patients with MAC-PD had significantly higher levels than patients with MAC contamination, those with pulmonary TB, those with other lung diseases, and healthy subjects—namely, 10.7 ± 7.9, 0.2 ± 0.1, 0.1 ± 0.1, 0.0 ± 0.1, and 0.0 ± 0.0 U/ml, respectively ($P < 0.0001$). A receiver operating characteristic (ROC) curve was constructed for MAC-PD and the other groups to establish the best cutoff value (Figure 2). Setting the cutoff value at 0.7 U/ml resulted in 100% specificity, at a sensitivity of 84.3% (Table E1). Using the EIA kit allowed clear discrimination between patients with MAC-PD and MAC contamination, pulmonary TB, and other lung diseases, as well as healthy subjects.

Next, we compared levels of serum IgA antibody to GPL core in fibrocavitary disease and NBE disease of MAC-PD. Significantly higher levels were found in NBE ($P < 0.05$) (Figure 3). With the cutoff value set at 0.7 U/ml, positivity in NBE and fibrocavitary disease was 91.4 and 63.2%, respectively. In contrast, in patients with MAC-PD, no significant differences between *M. avium* and *M. intracellulare* as causative agents were observed ($P = 0.403$). The erythrocyte sedimentation rate in MAC-PD was 32.6 ± 28.6 mm/hour and there was a significant positive correlation between the erythrocyte sedimentation rate and antibody levels in patients with MAC-PD ($r = 0.294$, $P < 0.05$).

Radiographic Severity and the Level of GPL Core Antibody

Forty-five patients with MAC-PD (10 with fibrocavitary disease, 26 with NBE disease, and 9 with unclassifiable type disease) underwent CCT and serodiagnosis at the same time. Four patients with unclassifiable type disease were excluded from the investigation because it was hard to discriminate between MAC lesions and underlying pulmonary disease. There was a positive correlation between the extent of disease and the

TABLE 1. CHARACTERISTICS OF STUDY SUBJECTS

	MAC-PD	MAC Contamination	Pulmonary TB	Other Lung Disease	Healthy Subjects
Number	70	18	36	45	76
Age, mean yr ± SD	68.0 ± 9.6	64.6 ± 11.6	52.9 ± 16.6*	66.3 ± 10.9	38.1 ± 12.0*
Age range, yr	50–90	28–78	24–76	29–82	20–65
Sex, no. male/no. female	25/45	10/8	26/10*	34/11*	41/35*
Duration of disease, mean yr ± SD	4.8 ± 4.6		0.3 ± 0.2	2.2 ± 2.4	

* $P < 0.001$.

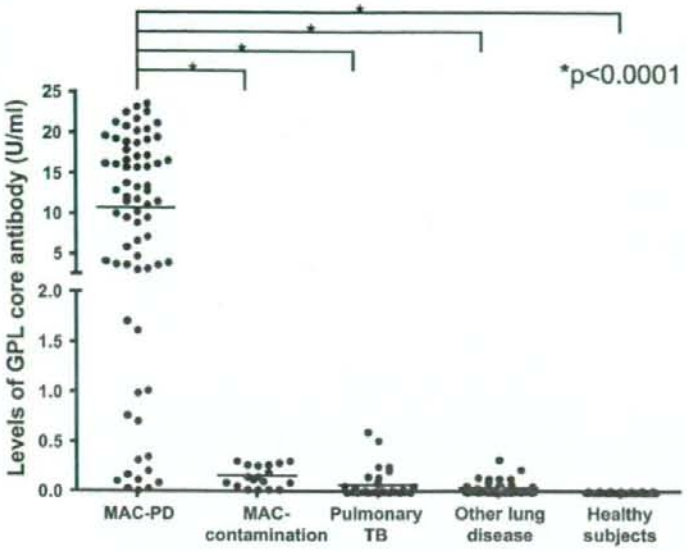

Figure 1. The level of serum IgA antibody to glycopeptidolipid (GPL) core antigen. Serum samples from six different institutions included 70 patients with *Mycobacterium avium* complex pulmonary disease (MAC-PD), 18 with MAC contamination, 37 with pulmonary tuberculosis (TB), 45 with other lung diseases, and 76 healthy subjects. Antibody levels in MAC-PD were significantly higher than in the other groups ($P < 0.0001$). All results are expressed as individual data, and *horizontal bars* indicate geometric means.

levels of the antibody ($r = 0.43$, $P < 0.05$) (Figure 4). The total numbers of involved segments were not different (7.8 ± 4.9 and 7.9 ± 4.2 in fibrocavitary and NBE disease, respectively). Of 26 patients with NBE disease, 9 had small thin wall cavities. A tendency toward elevated GPL core antibody levels was found in NBE patients with cavities compared with those without, but this trend was not statistically significant ($P = 0.08$).

DISCUSSION

We previously established a serologic test for MAC-PD using a mixture of GPLs and GPL core antigen, and reported the clinical application of the EIA method for quantifying antibody levels (7, 8). GPL is an antigen located on the surface of the MAC cell wall and determines the serotype. At present, 31 distinct serotype-specific GPLs have been identified, of which the complete structures of 14 have been identified (10–12). GPL consists of a core common to all MAC serotypes and a serotype-specific oligosaccharide. In the initial study to establish the serodiagnosis of MAC-PD, we used the whole GPL antigen, a mixture of 11 serotype-specific GPLs (7). We then found that the GPL core was the dominant antigenic epitope of GPL, and subsequently developed a serologic test using GPL core antigen (8). In the previous study, GPL core antibody (IgG, IgA, and IgM) levels were found to be elevated in sera of patients with MAC-PD, but not pulmonary TB, *M. kansasii*–PD, MAC colonization/contamination, and healthy subjects. The study showed that this serologic test was useful for diagnosing MAC-PD and for differentiating it from pulmonary TB and *M. kansasii*–PD. Consistent with this, Fujita and colleagues (13) reported elevated levels of antibody against the GPL core antigen in patients with MAC-PD but not in those with pulmonary TB. In our previous study (8), of the different Ig classes, best results were obtained by IgA, including an association with CCT findings. Thus, a higher level of serum IgA antibody to GPL core indicated a wider extent of MAC disease and larger nodule formation on CCT (9). Therefore, we have attempted to develop and to assess an EIA kit for quantifying serum IgA antibody to GPL core in the present study. Optical density levels were converted to U/ml using standard serum samples, which provided reliable and reproducible results. In this multicenter study, using the EIA kit, it was confirmed that patients with MAC-PD could be clearly differentiated from those with pulmonary TB, those with MAC contamination, those with other lung diseases, and healthy subjects. Similar to our previous studies (7–9), the sensitivity and specificity for diagnosing MAC-PD by the kit was high and the level of the antibody correlated with the extent of MAC-PD assessed using CCT.

Distinguishing pulmonary TB from MAC-PD in clinical practice using the EIA kit has proven useful. Differentiating TB from MAC is difficult because symptoms and radiographic findings are often similar among patients with pulmonary mycobacterial diseases. Patients with pulmonary TB require immediate treatment and isolation, whereas the diagnosis of MAC-PD does not necessitate rapidly starting antimicrobial therapy (1), and isolation is not required. GPL antigens, which are major cell surface antigens of MAC, are not present in the cell wall of *M. tuberculosis* complex (11). On the basis of this observation, patients with TB do not produce anti-GPL antibody. Indeed most patients with TB did not possess serum antibodies against GPLs (Figure 1) (7, 8). However, we cannot exclude the possibility that disease in patients with TB was of too short duration (MAC-PD, 4.8 ± 4.6 yr, vs. TB, 0.3 ± 0.2 yr) to have allowed immune responses and shed mycobacterial antigen. In this present study, with a cutoff level of 0.7 U/ml, all patients with TB were classified as seronegative. The levels of GPL core antibody in patients with pulmonary TB were very low or absent

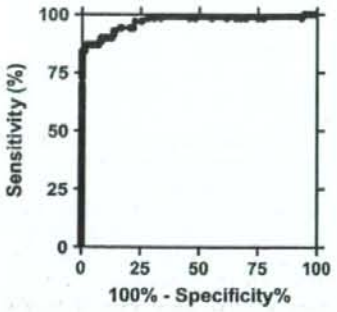

Figure 2. Receiver operating characteristic curve constructed for patients with *Mycobacterium avium*–complex pulmonary disease and the other groups.